

Planar contact geometry for far-infrared germanium lasers

D. R. Chamberlin,^{a)} E. Bründermann, and E. E. Haller^{b)}

Lawrence Berkeley National Laboratory and University of California, Berkeley, California 94720

(Received 18 January 1999; accepted for publication 25 April 1999)

We demonstrate operation of *p*-Ge far-infrared lasers with a planar contact geometry. The smallest laser crystal with this geometry has a maximum pulse length of 22 μ s, which is 10% longer than the pulse length of comparably doped lasers with the traditional contact geometry. Calculations of the electric field distribution show that the fraction of active crystal volume for this new geometry is \sim four times larger than that of traditional geometries. Experiments and calculations reveal that in the planar design, the minimum applied voltage necessary for lasing decreases when the crystal geometry approaches a flat planar structure. This is due to a significant increase of the total electric field caused by the Hall effect. © 1999 American Institute of Physics. [S0003-6951(99)01025-6]

A number of important applications exist for a compact, tunable, continuous-wave far-infrared (FIR) laser. For instance, astronomers need such a coherent source for high-resolution heterodyne spectroscopy of star-forming regions to determine chemical constituents, their distribution, and temperature redistribution.¹ A very promising device for such applications is the *p*-Ge laser operating with a hole population inversion. So far this device only works in a pulsed mode because the injected electrical power causes heating of the laser crystal above the maximum operating temperature in a few microseconds. Our objective is to achieve continuous-wave (cw) operation so that such a laser can be operated efficiently aboard satellites or high-altitude airborne observatories.

The *p*-Ge hole inversion laser operates near liquid helium temperatures in a perpendicularly crossed electric field *E* and magnetic induction *B*. Between a minimum and maximum *E/B* ratio, a population inversion is created between the light and heavy hole bands. In Ge:Be lasers this population inversion occurs under the condition $0.7 \text{ kV}/(\text{cmT}) \leq E/B \leq 2.0 \text{ kV}/(\text{cmT})$.² Far-infrared stimulated emission originates from transitions of holes between the light and heavy hole band or between light hole Landau levels. Because of the hole current necessary for operation, a large amount of resistive heating occurs. This increases the acoustic phonon density and at a certain temperature destroys the population inversion necessary for lasing. As a consequence *p*-Ge lasers currently must be operated in a pulsed mode.

Traditional *p*-Ge laser designs have two opposing p^+ -doped crystal faces completely covered with gold acting as ohmic contacts. These ohmic contacts also serve to connect the laser to a heat sink. However, the heat transfer is not efficient enough to allow cw operation. In order to reach cw operation, the ratio of input power to cooling surface must be reduced. This can be achieved by shrinking the crystal size.^{3,4} Recent studies have demonstrated operation of *p*-Ge lasers with volumes as small as 0.5 mm^3 .⁵ This study reported a maximum duty cycle of 2.5%, showing that additional improvement is necessary.

A further issue which was not addressed in Refs. 3 and 5 is the uniformity of the total electric field throughout the laser crystal volume. The total electric field E_T is the vector sum of the electric field generated by the externally applied voltage *U* and the Hall field from the applied magnetic induction *B* and the motion of the holes. The magnitude and orientation of E_T therefore depend strongly on *U*, *B*, the free carrier velocity, the laser crystal geometry, and the contact geometry. Detailed calculations have shown that only a fraction of the volume has the proper E_T .⁶ Experimental results have shown that increasing the electric field uniformity results in a narrowing of the laser line.⁷

The electric field uniformity turns out to be important for several reasons. First, the electric field determines the degree of Landau level mixing between light and heavy holes.⁸ Electric field variations within the laser crystal will result in several laser transitions with different energies, and gain will not be maximized for one particular frequency. Second, the light hole lifetime is dependent on the crystallographic orientation of E_T .⁹ Variations in the electric field will cause the light hole lifetime to change throughout the crystal. Finally, if the minimum E_T necessary for lasing is only met in a fraction of the laser crystal, the optically active volume is also only a fraction of the total, even though the entire crystal generates heat.

To evaluate the electric field uniformity we have solved the Poisson equation $\Delta\Phi = 0$ for this geometry with a finite difference technique considering the boundary conditions for those geometries in two dimensions.¹⁰ The space charge was assumed to be zero. The two ohmic contacts were fixed at potentials Φ_1 and Φ_0 . The other metal-free crystal surfaces have to comply with tangential current flow and the boundary conditions set by the Hall effect. With the vector **n** normal to the crystal surface, the current condition can be introduced by $\mathbf{I} \cdot \mathbf{n} = 0$. For a magnetic field in the *z* direction the Hall effect leads to a relation for the electric field components in the *x* and *y* direction. $E_x = \partial\Phi/\partial x$ and $E_y = \partial\Phi/\partial y$ are then a function of the tangent of the Hall angle α_H . In the calculation the maximum Hall angle given by $\alpha_H = \arctan(\pi/2) \approx 60^\circ$ was used which occurs for $E/B = 0.96 \text{ kV}/(\text{cmT})$.¹¹

The laser sample was not connected to a heat sink so that

^{a)}Electronic mail: drchamberlin@lbl.gov

^{b)}Electronic mail: eehaller@lbl.gov

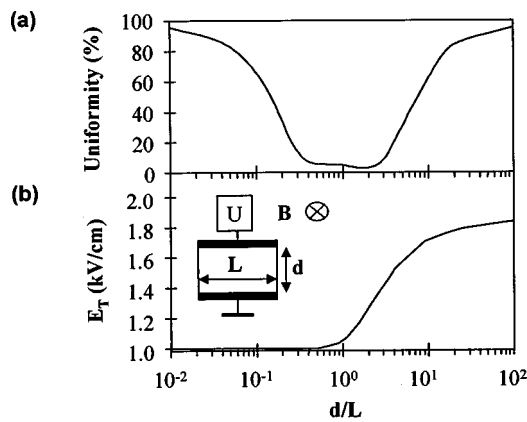


FIG. 1. (a) Electric field uniformity as a function of the ratio d/L where d is the distance between electrical contacts and L is the length in the direction of the Hall field. (b) Calculation of the total electric field E_T in the center of the laser crystal for a voltage U applied to the electrical contacts such that the applied electric field is 1 kV/cm. The conventional laser design is used.

an adiabatic heating process holds.^{5,12} Due to the high heat conductivity of Ge no thermal gradients are expected inside the laser. We therefore assume a position-independent mobility throughout the sample for our calculations. A detailed description of the theoretical model and potential and electric field line patterns are presented elsewhere.¹³

Figure 1(a) shows the percentage of the Ge laser crystal volume with E_T uniform to within $\pm 0.5\%$ as a function of the ratio of distance d between electrical contacts of the laser to length L in the direction of the Hall field, as obtained by finite-difference calculations. The value of $\pm 0.5\%$ used for Fig. 1 is chosen based on the distance between two heavy hole anticrossing points for the same light hole Landau level at $B = 0.7$ T.⁸ The percentage of the laser crystal with a uniform electric field reaches a maximum when the ratio d/L is either large or small, and is minimum when the ratio lies between 0.5 and 2. Unfortunately, recent experimental studies^{3,5,7} have focused on lasers with near-square cross sections ($d/L \approx 1$).

To increase the electric field uniformity, it is desirable to investigate laser designs with very large or very small d/L ratios. Figure 1(b) shows the calculated E_T in the center of the laser crystal for an externally applied bias field of 1 kV/cm and $\alpha_H \approx 60^\circ$. For $d/L \leq 0.5$, the electric field in the center of the laser is equal to the externally applied electric field. At a high d/L ratio, the Hall field plays a large role which means that the required E_T/B ratio can be achieved for a lower applied voltage and lower input power. However, this geometry has small electrical contact areas and a large distance between contacts. Since the heat sinks are attached to the electrical contacts, this design is disadvantageous for effectively cooling the laser.

To obtain a large d/L ratio, we have fabricated lasers with planar contact geometries as shown in Fig. 2(a). This design provides a relatively large contact size while allowing a large distance between contacts. The ohmic electrical contacts were oriented with the [001] direction normal to the contact surface. The magnetic field was pointed in the [110] direction, and the light was measured in the [110] direction perpendicular to B .

Ge single crystals were grown from a melt doped with

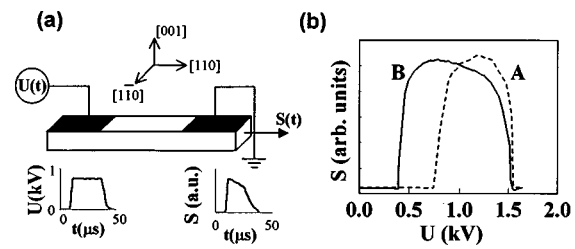


FIG. 2. (a) Geometry of the lasers used in this study with electrical contacts on the same Ge surface. The insets show an example of the voltage and optical pulse shapes for laser B. (b) Laser intensity S as a function of applied voltage U ; dashed line: laser A, solid line: laser B.

the double acceptor beryllium in a vacuum atmosphere using the Czochralski technique. The crystals were characterized with variable temperature Hall effect to determine the shallow acceptor and compensating donor concentrations. Lasers were fabricated by cutting the crystals with an ID saw and lapping the surfaces with 600 and 1900 grit SiC to create parallel crystal surfaces to within 30 arcsec. The lapped surfaces were polish etched in a 4:1 HNO_3 :HF or a 7:2:1 HNO_3 :HF:fuming nitric mixture. The Ge crystals were ion implanted on one surface with boron at a dose of $1 \times 10^{14} \text{ cm}^{-2}$ at 33 keV and $2 \times 10^{14} \text{ cm}^{-2}$ at 50 keV to form ohmic contacts. The implanted surfaces were sputter coated with 40 nm Pd and 400 nm Au, and annealed at 300 °C for 1 h to remove implantation damage. Two rectangular areas on the top of the laser crystal were masked with 5-mil-thick vinyl electrical tape and the gold layer between them was removed with an etching solution of 130 g KBr, 75 ml Br_2 , and 425 ml H_2O . The implant between the gold contacts was then removed by etching for 10 s in 4:1 HF: HNO_3 .

A pulse generator was used to apply voltage pulses of variable length (0.1–100 μs) and repetition rates (1 Hz–1 kHz). The circuit was designed to act as a constant voltage source during the pulse [Fig. 2(a)]. The sample resistance varies by only a few percent during the pulse which results in a similarly shaped, square current pulse. However, the optical pulse has a decay time due to heating,⁴ similar to laser pulse shapes obtained previously.⁵ The magnetic field was applied with two $20 \times 10 \times 10 \text{ mm}^3$ NdFeB permanent magnets with remanent magnetization $B_R = 1.2$ T separated by a distance of 3 mm which results in a magnetic induction of $B = 0.7$ T across the laser crystal. No external resonator cavity was used because the high refractive index of Ge allows operation using only the polished crystal surfaces as mirrors for internal reflections.

The laser emission was measured by a Ge:Al photoconductor immersed in liquid helium. The broadband laser emission is typically found in the frequency range from 70 to 90 cm^{-1} at $B = 0.7$ T,² close to the optimum sensitivity of the Ge:Al detector at 90 cm^{-1} . Since the photoconductor is completely bleached by the laser radiation, it cannot be used to measure the output power accurately. Assuming a typical efficiency for germanium lasers of 0.1%,¹⁴ the output power can be estimated at ~ 1 W.

Two lasers were fabricated from the same Ge crystal with a Be acceptor concentration of $7 \times 10^{13} \text{ cm}^{-3}$. Both lasers had an intercontact distance of 1 cm, however, laser A had a volume 4.2 times larger than laser B (see Table I). Not surprisingly, the maximum repetition rate was five times

TABLE I. Properties of lasers used in this study. L : length in $[110]$, w : width in $[1\bar{1}0]$, h : height in $[001]$, t_{\max} : maximum pulse length, ν_{\max} : maximum repetition rate at t_{\max} . No heat sinks were attached to the laser crystals.

	L (mm)	w (mm)	h (mm)	t_{\max} (μ s)	ν_{\max} (Hz)
Laser A	19.5	2.9	5	17	15
Laser B	12.8	2.4	2.2	22	75

larger for the smaller laser (B). However, the maximum pulse length of laser B was also 29% larger than for laser A. To first order one would expect that laser B would have a shorter pulse length because the smaller crystal size would lead to a smaller amplification.

The intensity of both lasers under an applied magnetic induction of 0.7 T was measured as a function of applied voltage. The normalized result is shown in Fig. 2(b). Laser B starts emitting at a lower threshold voltage, and can be operated at a lower electrical input power. This decreases the heating of the laser and explains the larger pulse length of the smaller crystal.

The electric field for the geometries of lasers A and B was calculated using the same finite difference method as for Fig. 1. The Hall angle, which is used as a boundary condition in the calculation, was used as a variable in Fig. 3(a). This calculation shows that for all Hall angles, E_T in the center of laser B will be larger than for laser A for the same applied bias. Laser B will reach the minimum electric field necessary for population inversion at a lower applied voltage than laser A.

Figure 3(b) shows the volume of laser crystal with an electric field within $\pm 0.5\%$ of the value in the center of the crystal. This calculation used a geometry with the same length L , width w , and distance between contacts d as laser B as a function of height h . A Hall angle of 60 degrees was used. There are two counteracting effects: as the height is increased from zero, the volume of uniform electric field increases because the total volume of the laser increases. At these low heights the field disturbance from the electrical contacts dominates the uniformity. The field disturbance penetrates into the center of the laser crystal to a distance of approximately one contact length, limiting the fraction of laser crystal with uniform volume to $\sim 60\%$. With further height increase the uniformity decreases further because of the asymmetric device geometry and the complex pattern of the Hall components on the Ge boundary surfaces. This re-

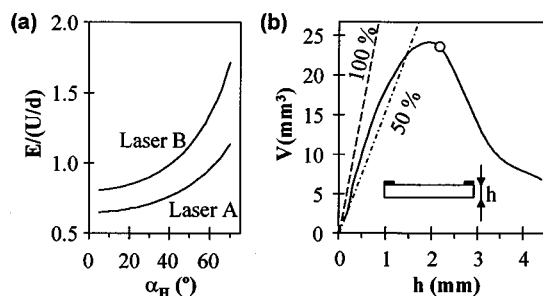


FIG. 3. (a) Calculation of the electric field in the center of the laser crystal as a function of the Hall angle α_H for a geometry with the same dimensions as lasers A and B. (b) Total crystal volume with a uniform electric field for a geometry with the same L and w as laser B as a function of h , for $\alpha_H = 60^\circ$. The data point corresponds to the dimensions of laser B.

sults in a peak in the total volume with uniform electric field at around 2 mm thickness, which is close to the geometry of laser B. From this calculation the fraction of laser crystal with a uniform electric field in laser B is 36%, which is much larger than the typical values for the near-cubic crystals used in Ref. 5 as seen from Fig. 1(a).

In summary, we have demonstrated operation of far-infrared p -Ge lasers with a new planar contact geometry. Finite difference calculations show that this geometry can result in a very uniform electric field distribution. Emission from lasers with this new design has shown a maximum pulse length of 22 μ s, exceeding the largest previously reported in the literature for a laser of the same doping concentration.⁵

Operation of p -Ge lasers in a planar geometry opens the door to many designs which will offer improved cooling possibilities. Lasers may be fabricated with an optically active doped layer on an undoped substrate, which would provide a heat sink with no thermal interface. Since the diffusivity of the triple acceptor Cu in Ge is high, these layers could easily be fabricated by diffusing Cu into ultrapure Ge at 700 $^\circ\text{C}$ to some limited depth. The diffusivity of Be and Zn are too low to make this method of fabrication practical for double-acceptor doped lasers. However, several hundred μm thick layers of Be-doped Ge could be grown on an undoped substrate by liquid phase epitaxy. We expect that the combination of increased electric field uniformity and cooling offered by this laser design will lead to cw operation in the near future.

The authors thank W. L. Hansen for the crystal growth and B. Tang for help with laser fabrication. We acknowledge partial support for this work by DLR, NE-WS, Berlin, and the use of facilities at the Lawrence Berkeley National Laboratory operated under U.S. Department of Energy Contract No. DE-AC03-76SF00098. D.R.C. acknowledges the NASA Office of Space Science Fellowship No. S98-GSRP-049 for their support. E.B. acknowledges support by the Alexander-von-Humboldt Foundation through a Feodor-Lynen Fellowship.

- R. T. Boreiko and A. L. Betz, *Astrophys. J., Suppl. Ser.* **111**, 409 (1997).
- L. A. Reichertz, O. D. Dubon, G. Sirmain, E. Bründermann, W. L. Hansen, D. R. Chamberlin, A. M. Linhart, H. P. Röser, and E. E. Haller, *Phys. Rev. B* **56**, 12069 (1997).
- E. Bründermann, A. M. Linhart, L. Reichertz, H. P. Röser, O. D. Dubon, W. L. Hansen, G. Sirmain, and E. E. Haller, *Appl. Phys. Lett.* **68**, 3075 (1996).
- P. D. Coleman and D. W. Cronin, *Int. J. Infrared Millim. Waves* **18**, 1241 (1997).
- E. Bründermann, D. R. Chamberlin, and E. E. Haller, *Appl. Phys. Lett.* **73**, 2757 (1998).
- R. C. Strijbos, J. E. Dijkstra, S. I. Schets, J. G. S. Lok, and W. T. Wenckebach, *Semicond. Sci. Technol.* **9**, 648 (1994).
- A. C. Bespalov and K. F. Renk, *Semicond. Sci. Technol.* **9**, 645 (1994).
- P. Pfeffer, W. Zawadzki, K. Unterrainer, C. Kremser, C. Wurzer, E. Gornik, B. Murdin, and C. R. Pidgeon, *Phys. Rev. B* **47**, 4522 (1993).
- S. A. Stoklitskiy, *Semicond. Sci. Technol.* **7**, B610 (1992).
- G. H. Shortley and R. Weller, *J. Appl. Phys.* **9**, 338 (1938).
- S. Komiyama, T. Masumi, and K. Kajita, *Phys. Rev. B* **20**, 5192 (1979).
- V. I. Gavrilenko, A. L. Korotkov, Z. F. Krasilnik, V. V. Nikornorov, and S. A. Pavlov, *Solid-State Electron.* **31**, 755 (1988).
- E. Bründermann, D. R. Chamberlin, and E. E. Haller, *Infrared Phys. Technol.* **40**, 141 (1999).
- F. Keilmann, V. N. Shastin, and R. Till, *Appl. Phys. Lett.* **58**, 2205 (1991).